Clinical Neurophysiology 133 (2022) 165–174

Contents lists available at ScienceDirect

Clinical Neurophysiology

journal homepage: www.elsevier.com/locate/clinph

High frequency oscillations associate with neuroinflammation in low-grade epilepsy associated tumors

Dongqing Sun [a,*], Nicole E.C. van Klink [a], Anika Bongaarts [b], Willemiek E.J.M. Zweiphenning [a], Maryse A van 't Klooster [a], Tineke A Gebbink [a], Tom J Snijders [a], Pieter van Eijsden [a], Pierre A.J.T. Robe [a], Eleonora Aronica [b,c], Maeike Zijlmans [a,c]

[a] Department of Neurology and Neurosurgery, UMC Utrecht Brain Center, University Medical Center Utrecht, Heidelberglaan 100, 3584CX Utrecht, the Netherlands
[b] Department of (Neuro)pathology, Amsterdam University Medical Centre, University of Amsterdam, Meijbergdreef 9, 1105AZ Amsterdam, the Netherlands
[c] Stichting Epilepsie Instellingen Nederland, Achterweg 2, 2103SW Heemstede, the Netherlands

See Editorial, pages 154–156

ARTICLE INFO

Article history:
Accepted 29 August 2021
Available online 18 October 2021

Keywords:
Epilepsy surgery
High frequency oscillations
Intraoperative electrocorticography
Neuroinflammation
Low-grade tumor

HIGHLIGHTS

- This is the first study to directly compare high frequency oscillations and inflammatory markers that contribute to epileptogenesis.
- Increased ripple rates correlate with increased IL1β/HMGB1/TLR4 pathway activity in the peritumoral tissue of low-grade tumors.
- Tumors that generate ripples are infiltrated by more CD3-positive T-cells than tumors without ripples.

ABSTRACT

Objective: High frequency oscillations (HFOs) in intraoperative electrocorticography (ioECoG) are thought to be generated by hyperexcitable neurons. Inflammation may promote neuronal hyperexcitability. We investigated the relation between HFOs and inflammation in tumor-related epilepsy.
Methods: We identified HFOs (ripples 80–250 Hz, fast ripples 250–500 Hz) in the preresection ioECoG of 32 patients with low-grade tumors. Localization of recorded HFOs was classified based on magnetic resonance imaging reconstructions: in tumor, in resected non-tumorous area and outside the resected area. We tested if the following inflammatory markers in the tumor or peritumoral tissue were related to HFOs: activated microglia, cluster of differentiation 3 (CD3)-positive T-cells, interleukin 1-beta (IL1β), toll-like receptor 4 (TLR4) and high mobility group box 1 protein (HMGB1).
Results: Tumors that generated ripples were infiltrated by more CD3-positive cells than tumors without ripples. Ripple rate outside the resected area was positively correlated with IL1β/TLR4/HMGB1 pathway activity in peritumoral area. These two areas did not directly overlap.
Conclusions: Ripple rates may be associated with inflammatory processes.
Significance: Our findings support that ripple generation and spread might be associated with synchronized fast firing of hyperexcitable neurons due to certain inflammatory processes. This pilot study provides arguments for further investigations in HFOs and inflammation.

1. Introduction

Epilepsy is thought to arise from uncontrollable neural excitation and epilepsy surgery can be an effective treatment for focal drug-resistant epilepsy (Ryvlin et al. 2014). One of the commonly encountered pathologies in epilepsy surgery practice are low-grade epilepsy-associated tumors (LEATs), mostly represented by

* Corresponding author at: University Medical Center Utrecht, Department of Neurology and Neurosurgery, Heidelberglaan 100, 3584CX Utrecht, the Netherlands.
E-mail address: d.sun-3@umcutrecht.nl (D. Sun).

https://doi.org/10.1016/j.clinph.2021.08.025
1388-2457/

glioneuronal tumors (Blumcke et al. 2017; Blümcke et al. 2019; Slegers and Blumcke 2020). Surgical removal of LEAT itself does not always suffice to achieve favorable seizure outcome (Englot et al. 2012; Lamberink et al. 2020). The epileptogenic zone often extends further than the visible lesion and the epileptogenic effect takes place both inside and outside the tumor (Thom et al. 2012; Giulioni et al. 2017).

Promising interictal electroencephalographic biomarkers for identifying epileptogenic tissue are high frequency oscillations (HFOs, ripples: 80–250 Hz; fast ripples (FRs) 250–500 Hz) (Jacobs et al. 2008; Zijlmans et al. 2012; van 't Klooster et al. 2017). HFOs in intraoperative electrocorticography (ioECoG) can be recorded over and around the lesion and may be used to delineate the epileptogenic tissue (van 't Klooster et al. 2017). Resection of the HFO-rich area has been associated with good seizure outcome and the presence of postoperative FRs predicts seizure recurrence (Wu et al. 2010; Fujiwara et al. 2012; van 't Klooster et al. 2017). HFO generation involves multiple mechanisms. On a cellular level, it has been proposed that HFOs mainly reflect action potentials of neurons and could be generated by synchronized fast firing of interconnected hyperexcitable neurons (Jiruska et al. 2017).

Neuronal hyperexcitability can be caused by inflammation. Proinflammatory molecules, activated microglia and other inflammatory components are found in and around epileptic lesions and contribute to epileptogenesis by increasing neuronal excitability and decreasing seizure threshold (Boer et al. 2008; Vezzani and Friedman 2011; Vezzani et al. 2011a, 2013). Activation of the concomitant interleukin-1 beta (IL1B)/ toll-like receptor 4 (TLR4)/ high mobility group box 1 protein (HMGB1) pathway induces functionality changes in microglia, astrocytes and neurons as well as promoting neuronal hyperexcitability (Vezzani et al., 2011b; Shimada et al., 2014).

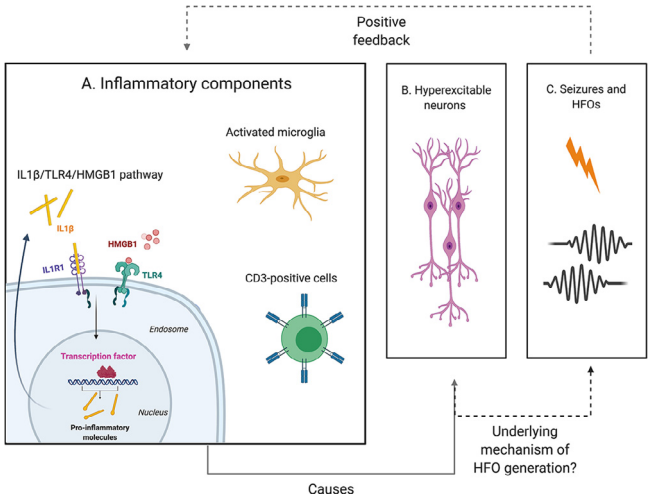

Fig. 1. Hypothesized relation between HFOs and neuroinflammation. Inflammation could promote neuronal excitability and decrease seizure threshold. HFOs are biomarkers for epilepsy and may be generated by synchronized fast firing of hyperexcitable neurons. Therefore, we hypothesized that HFOs may be associated with inflammatory markers. A. Inflammatory components investigated in this study: activated microglia, CD3-positive T-cells and the IL1β/TLR4/HMGB1 pathway. A short description of the IL1β/TLR4/HMGB1 pathway: IL1β binds to the interleukin-1 receptor-1; HMGB1 binds to TLR4. Activation of the concomitant IL1β/TLR4/HMGB1 pathway induces transcriptional factors and consequently the expression of pro-inflammatory mediators. B. Neuroinflammation could lead to neuronal hyperexcitability. C. Fast firing of hyperexcitable neurons is associated with epileptogenic HFO generation and epileptogenesis. Seizures stimulate inflammatory processes and hereby form a positive feedback loop. Abbreviations: HFO = High frequency oscillation, CD3 = cluster of differentiation 3, IL1β = interleukin 1-beta, TLR4 = toll-like receptor 4, HMGB1 = high mobility group box 1 protein.

We hypothesized that the epileptogenic mechanism of neuroinflammation might correspond to the pathophysiology behind HFO generation (Fig. 1). Understanding the relation between HFOs and inflammation markers in brain tissue could provide insights in the pathophysiological mechanism behind HFO generation and epileptogenesis. In this pilot study, we investigated the correlation between HFOs and inflammation markers known to contribute to epileptogenesis in patients with LEATs who underwent epilepsy surgery.

2. Methods

2.1. Patient selection

Patients who underwent epilepsy surgery with ioECoG at 2048 Hz sampling frequency due to LEAT (pathology confirmed) at the University Medical Centre Utrecht between 2008 and 2016 were included if the following data were available: 1) ioECoG recordings before tumor resection, 2) documentation of ioECoG positions, 3) pre- and postoperative MRIs, and 4) pathology specimen available for analyses. Patients with ioECoG with a high level of high frequency noise were excluded. These patients were also included in a retrospective study on HFOs and seizure outcome (van Klink et al. 2021).

2.2. Medical ethical approval

The institutional ethical committee approved the study and waived the need for written informed consent because of the retrospective character of the study if data were coded and handled pseudo-anonymously. Tissue for additional pathology analysis was obtained and used in accordance with the Declaration of Helsinki and the Research Code provided by the Medical Ethics Committee of both University Medical Center Utrecht and Amsterdam Medical Center. Tissue usage was approved by the review board of the University Medical Center Utrecht Biobank.

2.3. Intraoperative electrocorticography and clinical data

Epilepsy surgery was performed under general anesthesia with propofol. IoECoG was used to delineate the epileptogenic tissue and for functional cortical mapping when necessary. IoECoG was recorded directly on the cortex with 4x8 or 4x5 electrode grids and 1x6 or 1x8 electrode strips (Ad-Tech, Rachine, WI, USA). The silicone grids and strips embedded platinum electrodes with 4.2 mm^2 contact surface with 1 cm inter-electrode distance. Strip electrodes were used to record signals from the mesial and subtemporal area. The location of the grids and strips was captured with photographs. Signals were recorded with a 64-channel EEG system (Micromed, Veneto, Italy), at a 2048 Hz sample frequency with a low pass filter of 538 Hz. Propofol was stopped before each ioECoG recording to achieve a continuous background pattern with minimal propofol effect while the patients remained asleep. The surgical resection was determined based on MRI findings, interictal spikes and spike patterns in the ioECoG. Clinical data were available from medical reports. We collected seizure frequency from the most recent data available prior to surgery. If patients had different types of seizures with different seizure frequencies, the mean seizure frequency was calculated. We quantified semiquantitative descriptions, e.g. 'a couple of seizures' were quantified as 2–3 seizures. Seizure outcome was assessed according to the Engel classification at longest follow-up available. We classified patients with an Engel outcome 1A – 1B as seizure free and those with 1C – 4 as having recurrent seizures (Engel et al. 1993).

2.4. Electrode position

IoECoG electrode positions were reconstructed on the rendering of the cortical surface with 3D Slicer (V4.5.0–1). The cortex rendering was based on presurgical 3D T1 MRI with SPM 12 and 3D Slicer. We segmented the tumor in a presurgical 3D FLAIR MRI (1x1x1 mm) and the resected area in a postsurgical MRI (usually 3D T1, 0.6x0.6x0.6 mm). The presurgical and postsurgical MRIs were merged to determine the overlap of the tumor and the resected area. The ioECoG electrodes were reconstructed on the merged MRI rendering. The location of the electrodes on the cortex were determined by matching the gyral pattern of intraoperative photos of the grids to the cortical rendering (Fig. 2). We determined which contacts of the grids and strips were positioned on the tumor. Bipolar montages of the electrodes were defined as being located on tumor, on non-tumoral tissue that was resected, or outside the resection area (non-resected). For mesial temporal located tumors, the contacts covering the tumor were located on a strip that was slid under the temporal lobe and were out of sight for the surgeon. The first three strip electrodes were defined as being on the tumor.

2.5. HFO analyses

We selected one-minute epochs of each ioECoG preceding the resection that were free from large artefacts and with minimal propofol effects. Data were analyzed in a bipolar montage using an automated HFO detection algorithm (Burnos et al. 2014) adapted for our own ioECoG data. Every detected HFO was visually checked in Stellate Harmonie Reviewer (v7.0, Montreal, QC, Canada) by two out of the three reviewers (NvK/WZ/MZ). We used a split screen to visualize ripples (high pass FIR filter at 80 Hz, gain of 5 μV/mm, 0.4 s/page) and FRs (high pass finite impulse response filter at 250 Hz, gain of 1μVmm and 0.4 s/page). We analyzed all recordings preceding the resection. Multiple grid placements could overlap. If the same brain area is measured multiple times, we calculated the mean number of events for that location. HFO rate was defined as the number of ripples or FRs per minute. The total HFO rate was determined for each patient over all locations ($R_{total,}$ FR_{total}). Then we classified the location of the HFOs according to electrode positions determined on the MRI reconstruction: (a) HFO rate over the tumor site (R_{tumor}, FR_{tumor}), (b) HFO rate over resected area which was not tumorous according to the MRI ($R_{resection}$, $FR_{resection}$) and (c) HFO rate outside the resected area ($R_{non\text{-}resected}$, $FR_{non\text{-}resected}$).

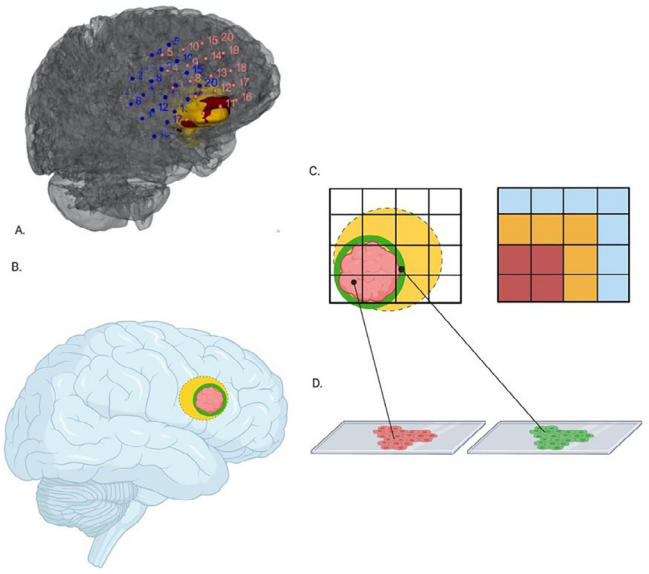

Fig. 2. Reconstruction of the ioECoG position and its relation to the tissue samples. A) Example of an MRI reconstruction from a patient included in this study. Red indicates the tumor and yellow indicates the resected tissue. Two grid recordings were performed and the electrode locations were reconstructed. B) Schematic representation of the MRI reconstruction. The tumor (red) located in the right frontal area. Peritumoral inflammation is around the tumor (green). Yellow represents the resected brain tissue that appeared normal on the MRI (resected area). The non-resected area is marked in blue. C) The ioECoG were divided into three areas based on their coverage: tumor (red), resected non-tumoral area (yellow) and non-resected tissue (blue). If multiple grids overlapped in position, we calculated the mean number of events for every location. D) Inflammation status was assessed for two areas: the tumor tissue (red) or the peritumoral area (green). Abbreviations: ioECoG = intraoperative electrocorticography; MRI = magnetic resonance imaging.

2.6. Pathology

We investigated the following markers of inflammation: microglia (HLA-DR (CR3/43) and CD3-positive cells, and IL1β/HMGB1/TLR4. In addition, we analyzed the v-raf murine sarcoma viral oncogene homolog B1 p.Val600Glu ($BRAF^{V600E}$) alterations and the isocitrate dehydrogenase (IDH) alterations. All tumor cases were reviewed independently by two neuropathologists, and the diagnosis was confirmed according to the revised WHO classification of tumors of the central nervous system (Louis et al. 2016); Additional molecular diagnosis was performed on LEAT samples with enough DNA to identify mutations in BRAF (Thom et al. 2018). Brain tissue from tumor patients was fixed in 10% buffered formalin and embedded in paraffin. Paraffin-embedded tissue was sectioned at 5 μm, mounted on pre-coated glass slides (Star Frost, Waldemar Knittel GmbH, Brunschweig, Germany). One representative paraffin block per case was sectioned, stained and assessed. Single-label immunohistochemistry was performed, as previously described (Prabowo et al. 2015; Bongaarts et al. 2020). The following antibodies were used: anti-human leukocyte antigen (HLA)-DP, DQ, DR (mouse clone CR3/43; DAKO; 1:100), CD3 (mouse monoclonal, clone F7.2.38, DAKO, 1:200; T-lymphocytes), toll-like receptor 4 (TLR4, polyclonal rabbit, sc10741, Santa Cruz, 1:20), IL1β (polyclonal goat IgG, Goat anti-human Il-1β antibody (C-20), Santa Cruz, 1:70), and HGMB1 (polyclonal rabbit, Ambcam, 1:1000). Hereafter, sections were washed in PBS and stained with a polymer-based peroxidase immunocytochemistry detection kit (PowerVision Peroxidase system, ImmunoVision, Brisbane, CA, USA).

Sections of all specimens were processed for hematoxylin and eosin (HE), and for immunocytochemical stainings for several neuronal and glial markers, and Ki67 (as marker of cell proliferation) to confirm the diagnosis of ganglioglioma or dysembryoplastic neuroepithelial tumors. All labelled tissue sections were evaluated by two independent observers blinded to clinical data for the presence or absence of various histopathological parameters and specific immunoreactivity (IR) for the different markers. We semi-quantitatively evaluated the IR for CD3. The intensity of HLA-DR (MHC-II), IL-1β, TLR4 and HMGB1 immunoreactive staining was evaluated using a scale of 0–3 (0: -, no; 1: +/-, weak; 2: +, moderate; 3: ++, strong staining). All areas of the tumors and the peritumoral cortex were examined and the score represents the predominant cell staining intensity found in each case. The expression of IL1β and TLR4 was analyzed both in neuronal and glial cells. The frequency of HLA-DR, IL1β, TLR4 and HMGB1 positive cells [(1) rare; (2) sparse; (3) high] was evaluated to give information about the relative number of positive cells within and around the tumor. As proposed before (Prabowo et al. 2015), the product of these two values (intensity and frequency scores) was taken to give the overall score (total score; total score; immunoreactivity score; IRS).

2.7. Statistical analyses

We used non-parametric statistical methods, because our data were not normally distributed. We reported continuous variables as medians with interquartile ranges (IQR) and categorical variables as frequencies and percentages (%). Differences between two continuous variables were tested with the Wilcoxon Signed Rank test (2 related samples) or Mann-Whitney U test (2 independent samples). We performed Spearman's Rho correlation test correlation analyses for the following variables:

- Inflammation markers × inflammation markers
- Ripple rate or FR rate × inflammation markers in tumor tissue
- Ripple rate or FR rate × inflammation markers in peritumoral tissue

We performed standard multiple regression analyses if the assumptions for this analysis were met. A p-value < 0.05 was considered statistically significant. Statistical analysis was performed in IBM SPSS Statistics 26 (IBM Corp., Armonk, NY). We did not correct for multiple comparison because we deemed that the relevance of reporting all potential effects transcends the importance of avoiding type I errors in this explorative study.

3. Results

3.1. Patient population

Thirty-two patients who underwent epilepsy surgery due to LEAT (confirmed by pathology) with ioECoG (sampled at 2048 Hz) were included (Table 1). All lesions were macroscopically completely resected. Twenty-four patients were seizure free after surgery and eight patients had recurrent seizures. All 32 surgical specimens contained sufficient tumoral tissue for analyses. Eighteen specimens contained sufficient peritumoral tissue (normal-appearing cortex/white matter adjacent to the tumor). Based on the pathological hallmarks diagnosis was set for ganglioglioma in 26 patients, desmoplastic infantile ganglioglioma in one patient and desembryoplastic neuroepithelial tumor in 5 patients. The HFO rates were not significantly different between the pathologies. All tumors were IDH wild type. 18 tumors had $BRAF^{V600E}$ mutations. The HFO rates were not significantly different between $BRAF^{V600E}$ mutated and $BRAF^{V600E}$ wild type tumors.

3.2. IoECoG analyses

1326 bipolar electrodes in ioECoG were analyzed. Ripples were present in the ioECoG of 30 patients with a median ripple rate in this ripple-positive group of 21.5/min, IQR [7.5 – 48.5]. The ripple rate was the highest outside the resected area which was significantly higher than in the tumor (7.8/min vs. 1.3/min, Z = -2.54, p = 0.01) (Fig. 3A). FRs were found in the ioECoG of 10 patients with a median FR rate of 14.5/min, IQR [4.8 – 32.8]. Most FRs were found in the resected area. The FR rate in the resected area was similar to the FR rate in the tumor but significantly higher than the FR rate outside the resection (8.0/min vs. 0.0/min, Z = -2.38, p = 0.02) (Fig. 3B). Preoperative HFO rates were not significantly different between seizure free patients and patients with recurrent seizures.

3.3. Inflammatory status

The IRS of IL1β, TLR4, HMGB1 and HLA-DR and the number of CD3-positive cells is presented in the Supplement (Supplementary Table 1). The tumor tissue expressed significantly higher IRS of IL1β, TLR4, HMGB1 and HLA-DR than the peritumoral tissue (all p < 0.001, Fig. 4). The number of CD3-positive cells was higher in the tumor tissue than the peritumoral tissue (U = -3.76, p < 0.001, Fig. 4). IRS of TLR4 in the peritumoral neurons correlated positively with presurgical seizure frequency (Spearman's rho = 0.54, p = 0.02). Other inflammatory markers did not correlate with seizure frequency. The expression of the inflammatory markers in the tumor and the peritumoral tissue was not significantly different between the seizure free and the seizure recurrent group.

3.4. HFO rate and inflammation

Patients with ripples in their ioECoG had more CD3-positive cells infiltrating the tumor tissue than patients without ripples (U = 3.5, p = 0.03). When looking at different locations in ioECoG, more CD3-positive cells were found in the tumors that showed ripples than the tumors without ripples (U = 66.5, p = 0.023). The number of CD3-positive cells was not significantly different between patients with and without FRs. Patients with ripples outside the resected area had higher immunoreactivity of $IL1\beta_{peri}$ (U = 5.0, p = 0.037), $TLR4_{peri}$ (U = 2.00, p = 0.014) and $HMGB1_{peri}$ (U5.5, p = 0.041) than those without ripples. The correlation analyses demonstrated that increased ripple rate outside the resected area correlated with increased immunoreactivity of $IL1\beta_{peri}$ (Spearman's rho = 0.57, p = 0.01) and $TLR4_{peri}$ (Spearman's rho = 0.62, p = 0.007) in the peritumoral glia cells (Fig. 5B and 6). Increased ripple rates outside the resected area were correlated with increased immunoreactivity of $HMGB1_{peri}$ in de peritumoral tissue (Spearman's rho = 0.58, p = 0.01, Fig. 5B and Fig. 6). FRs did not correlate with inflammatory markers (Fig. 5C and D).

4. Discussion

We investigated the correlation between HFOs in ioECoG and inflammation markers involved in epileptogenesis (IL1β, TLR4, HMGB1, HLA-DR and CD3). In the ioECoG of patients who underwent epilepsy surgery due to low-grade tumors, ripples were present in 30 patients and FRs in ten patients. The HFO rate were determined in the ioECoG covering the tumor, the resected non-tumorous tissue and outside the resected area. Tumor tissue that showed ripples was infiltrated by more CD3-positive T-cells than tumor tissue without ripples. Outside the resected area, increased ripple rate was positively correlated with increased immunoreactivity of IL1B, TLR4 and HMGB1 in the peritumoral tissue. In other words, the higher the ripple rate outside the resected area, the more the concomitant IL1β/HMGB1/TLR4 pathways were active in the peritumoral tissue. Other studies suggested a link between ripples and epileptogenicity and a link between inflammation and epileptogenicity (Zijlmans et al., 2012; Vezzani et al., 2013; van Vliet et al., 2018). In our data, the immunoreactivity of TLR4 in peritumoral neurons correlated positively with presurgical seizure frequency. We found a link between ripples and inflammation which could either represent a direct relationship or indirectly support their mutual association with epileptogenicity. FR rate did not correlate with inflammation, but the number of patients with fast ripples was too small to draw conclusions.

We expected a positive correlation between ripple rate and IL1β/HMGB1/TLR4 because IL1β/HMGB1/TLR4 pathway activation promotes neuronal hyperexcitability which corresponds to the pathophysiology behind ripple generation. We found that only ripple rates in the non-resected area were positively correlated with the immunoreactivity of IL1β/HMGB1/TLR4 in the peritumoral tissue. The non-resected area and the peritumoral tissue did not overlap in precise location. The associations might be explained in two ways: 1) the expression of the inflammatory markers outside the resected area cannot be measured. The IRS of IL1β in the peritu-

Table 1
Patient characteristics.

Case	Gender & age	Tumor location & pathology	Seizure outcome[1] & follow-up[2]	Number of electrodes	HFO rate[3]		IDH	$BRAF^{V600E}$ mutation
1	M	Frontal R	2B	13	R	0	WT	N
	12	DIG	78		FR	0		
2	F	Temporal R	1D	57	R	4	WT	Y
	28	GG	27		FR	0		
3	M	Mesiotemporal L	1A	35	R	121	WT	Y
	20	GG	94		FR	44		
4	F	Mesiotemporal R	3A	32	R	23	WT	Y
	16	GG	53		FR	0		
5	F	Frontal R	1A	65	R	18	WT	N
	13	GG	10		FR	0		
6	M	Temporal L	1D	36	R	15	WT	Y
	28	GG	50		FR	9		
7	M	Mesiotemporal R	1A	37	R	133	WT	N
	6	GG	45		FR	29		
8	M	Mesiotemporal R	1A	110	R	458	WT	Y
	24	GG	50		FR	67		
9	M	Mesiotemporal L	1A	37	R	13	WT	Y
	11	GG	56		FR	0		
10	M	Mesiotemporal R	1A	19	R	39	WT	Y
	0	GG	45		FR	0		
11	F	Temporal L	1C	62	R	47	WT	Y
	13	GG	40		FR	19		
12	F	Mesiotemporal L	1A	35	R	21	WT	Y
	10	GG	15		FR	0		
13	M	Mesiotemporal R	1C	37	R	14	WT	N
	23	GG	38		FR	0		
14	F	Mesiotemporal L	1A	32	R	48	WT	Y
	15	GG	25		FR	0		
15	M	Temporal R	1A	37	R	50	WT	N
	19	DNET	26		FR	10		
16	F	Temporal L	1A	62	R	2	WT	N
	12	DNET	24		FR	0		
17	F	Temporal L	1B	55	R	3	WT	Y
	16	GG	16		FR	0		
18	F	Temporal R	1D	28	R	33	WT	N
	16	GG	14		FR	3		
19	M	Pariental R	4B	16	R	0	WT	N
	50	DNET	30		FR	0		
20	M	Frontal R	1A	49	R	3	WT	N
	14	GG	27		FR	0		
21	M	Mesiotemporal R	1A	29	R	9	WT	Y
	11	GG	19		FR	0		
22	F	Mesiotemporal R	1A	18	R	22	WT	Y
	2	GG	21		FR	0		
23	F	Mesiotemporal R	1A	37	R	3	WT	N
	16	DNET	15		FR	0		
24	F	Temporal L	1A	40	R	88	WT	Y
	4	DIG	15		FR	26		
25	F	Mesiotemporal R	1A	36	R	70	WT	Y
	3	GG	15		FR	5		
26	M	Frontal L	1A	46	R	92	WT	N
	17	GG	16		FR	0		
27	M	Temporal R	1A	34	R	8	WT	Y
	12	GG	14		FR	0		
28	F	Temporal R	1A	56	R	24	WT	N
	13	DNET	11		FR	0		
29	F	Mesiotemporal L	1A	30	R	26	WT	Y
	13	GG	15		FR	4		
30	M	Temporal L	1A	71	R	1	WT	N
	10	GG	13		FR	0		
31	F	Temporal R	1A	46	R	14	WT	Y
	31	GG	11		FR	0		
32	M	Temporal R	1A	29	R	8	WT	N
	20	GG	15		FR	0		

Abbreviations: M = male, F = female, age = age in years, DIG = desmoplastic infantile ganglioglioma, GG = ganglioglioma, DNET = dysembryoplastic neuroepithelial tumor, HFO = high frequency oscillation, R = ripple, FR = fast ripple, IDH = isocitrate dehydrogenase, WT = wild type, $BRAF^{V600E}$ = v-raf murine sarcoma viral oncogene homolog B1 p. Val600Glu, Y = yes, N = no. [1] = seizure outcome according to the Engel classification (Engel et al. 1993), [2] = follow-up period in months, [3] = number of high frequency oscillations per minute.

moral tissue does not preclude a diffusion of this cytokine towards the areas where the ripples are found as the IRS can only detect the cells producing interleukins and not the soluble and extracellular interleukins. 2) Ripples outside the resected tissue could be propagated from the tumor and resected area, the areas where the inflammatory markers were analyzed. In that case, one would also

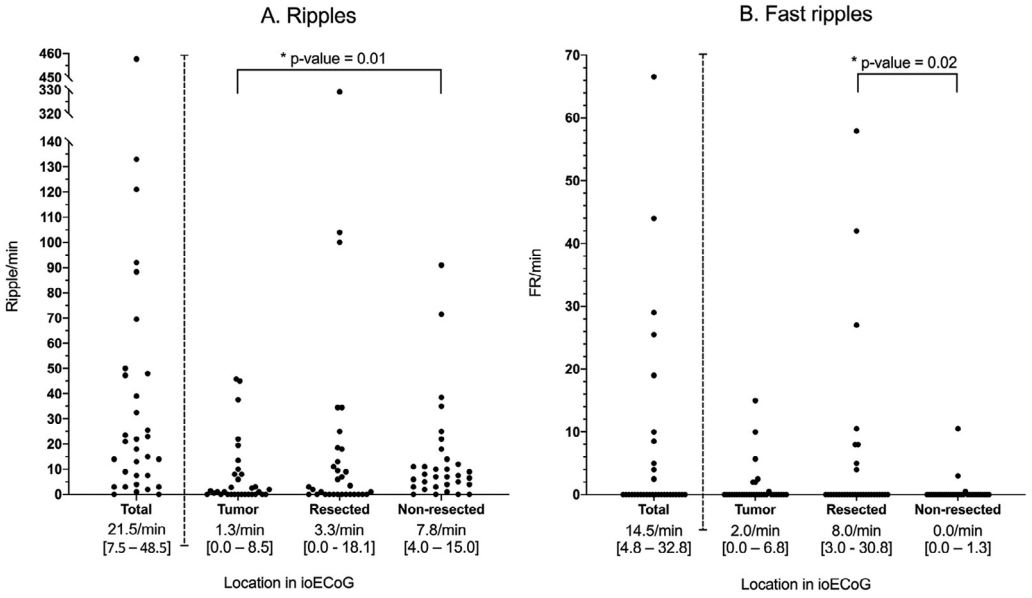

Fig. 3. Distribution of HFO in different locations of the ioECoG. The total HFO rate in the whole grid and the HFO rate in different locations covering the tumor, resected and non-resected region (A: ripples, B: FRs). Each dot represents the HFO rate of an individual patient. Median and interquartile range is given for patients with HFOs present in the ioECoG. Abbreviations: min = minute, * = statistical significant difference ($p < 0.05$).

expect an association between ripple rate in the tumor and the resected area with inflammation. The absence of such association might be because the ripple rates in these areas were less distributed between patients and thus limited the power of the correlation analyses. The combination of these two factors might explain why association exists between ripple rate and inflammation in two different areas in the brain.

High number CD3-positive T-cell infiltrating in the tumor was also associated with presence of ripples in the tumor. This finding might suggest that the activation of the adaptive immune system could support epileptogenesis and ripple generation. The immunoreactivity of HLA-DR did not relate to the ripple rates, despite the role of microglia in the IL1B/HMGB1/TLR4 pathway. This could be due to the versatile role of microglia in LEAT related

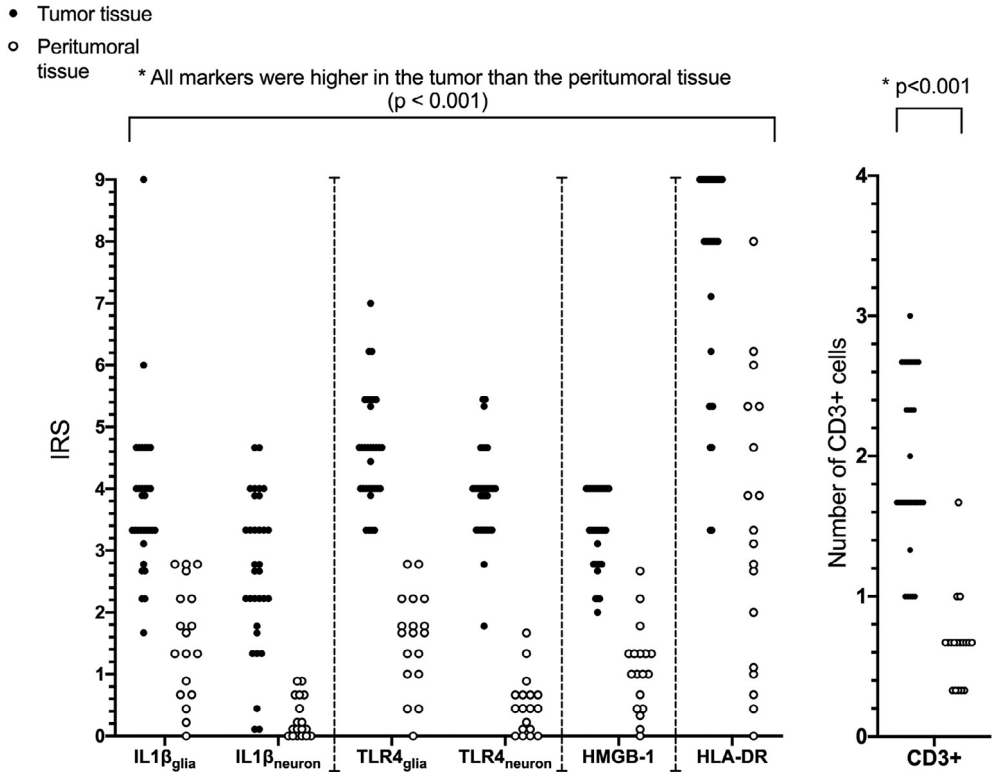

Fig. 4. Inflammatory markers. Inflammatory markers in the tumor tissue (black dots) and peritumoral tissue (white dots) expressed in immunoreactivity score (IL1β, TLR4, HMGB1, HLA-DR) or the number of CD3-positive cells. Abbreviations: IRS = immunoreactivity score, glia = in glia cells, neuron = in neuronal cells, CD3 = cluster of differentiation 3, IL1β = interleukin 1-beta, TLR4 = toll-like receptor 4, HMGB1 = high mobility group box 1 protein, * =statistical significant difference ($p < 0.05$).

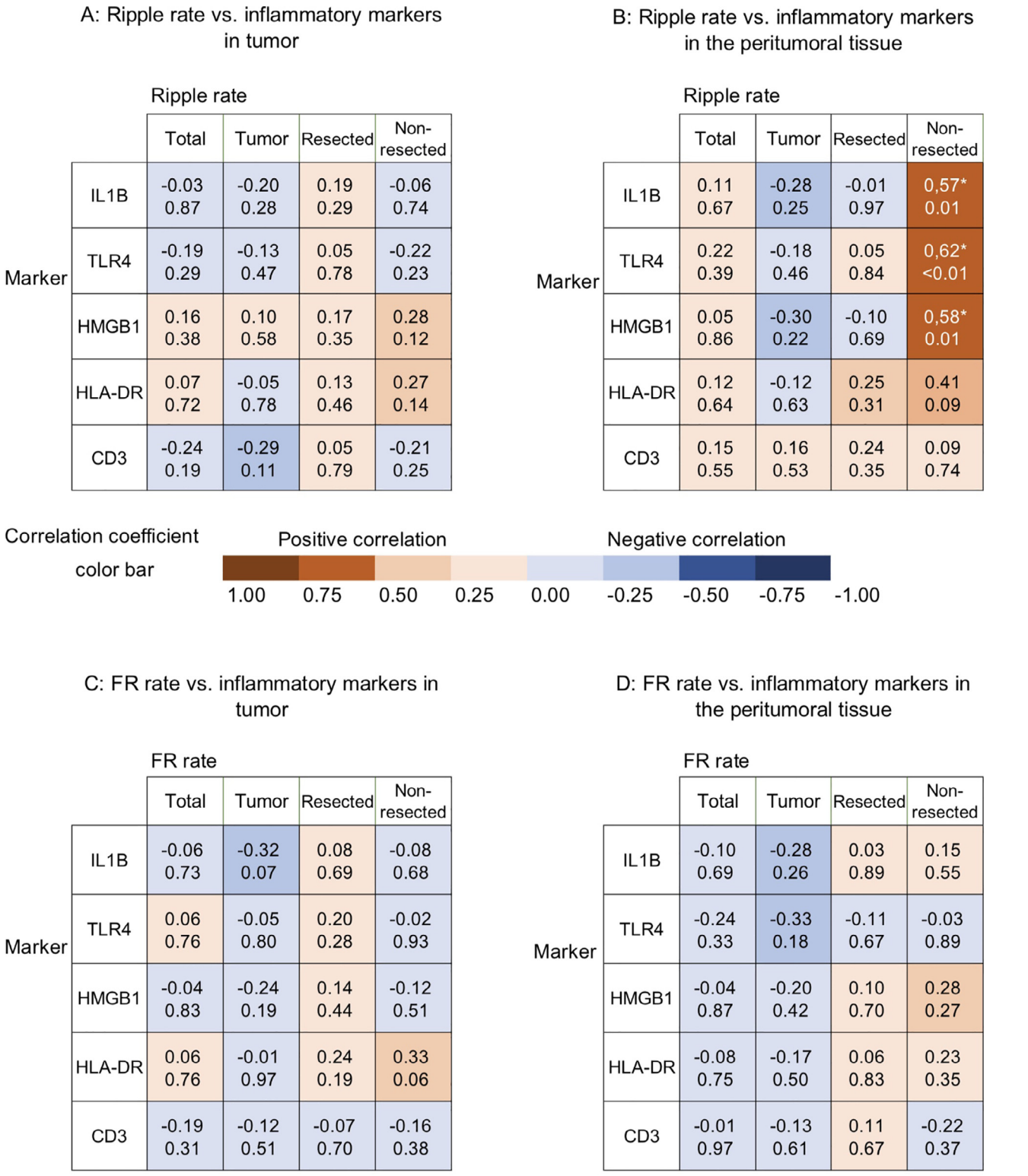

Fig. 5. Correlation matrix of HFOs vs. inflammatory markers. Correlation matrix of HFO rate and inflammatory makers represented with color chart. The first row represents the Spearman's Rho correlation coefficient and the second row represents the p-value. The color intensity corresponds with the correlation coefficient and is shown in the correlation coefficient color bar. A: ripple rate vs. inflammation in the tumor tissue and B: ripple rate vs. inflammation in the peritumoral tissue. C: FR rate vs. inflammation in the tumor tissue and D: FR rate vs. inflammation in the peritumoral tissue. Abbreviations: HFOs = high frequency oscillations, FR = fast ripples, vs = versus,* = statistical significance $p < 0.05$.

epilepsy; activated microglia are not only important immune players, but also regulators of tumor proliferation and invasion (Graeber et al. 2002; Aronica et al. 2005).

FR rates did not correlate with inflammatory markers. FRs were recorded in a small group of patients and the FR rates were generally low. Therefore, our observations could not exclude any association between FRs and inflammatory markers with certainty. In addition, FRs and ripples have different pathophysiological mechanisms. FR generation does not rely on synchronized firing of neurons alone, but also involves out-of-phase firing of neuronal

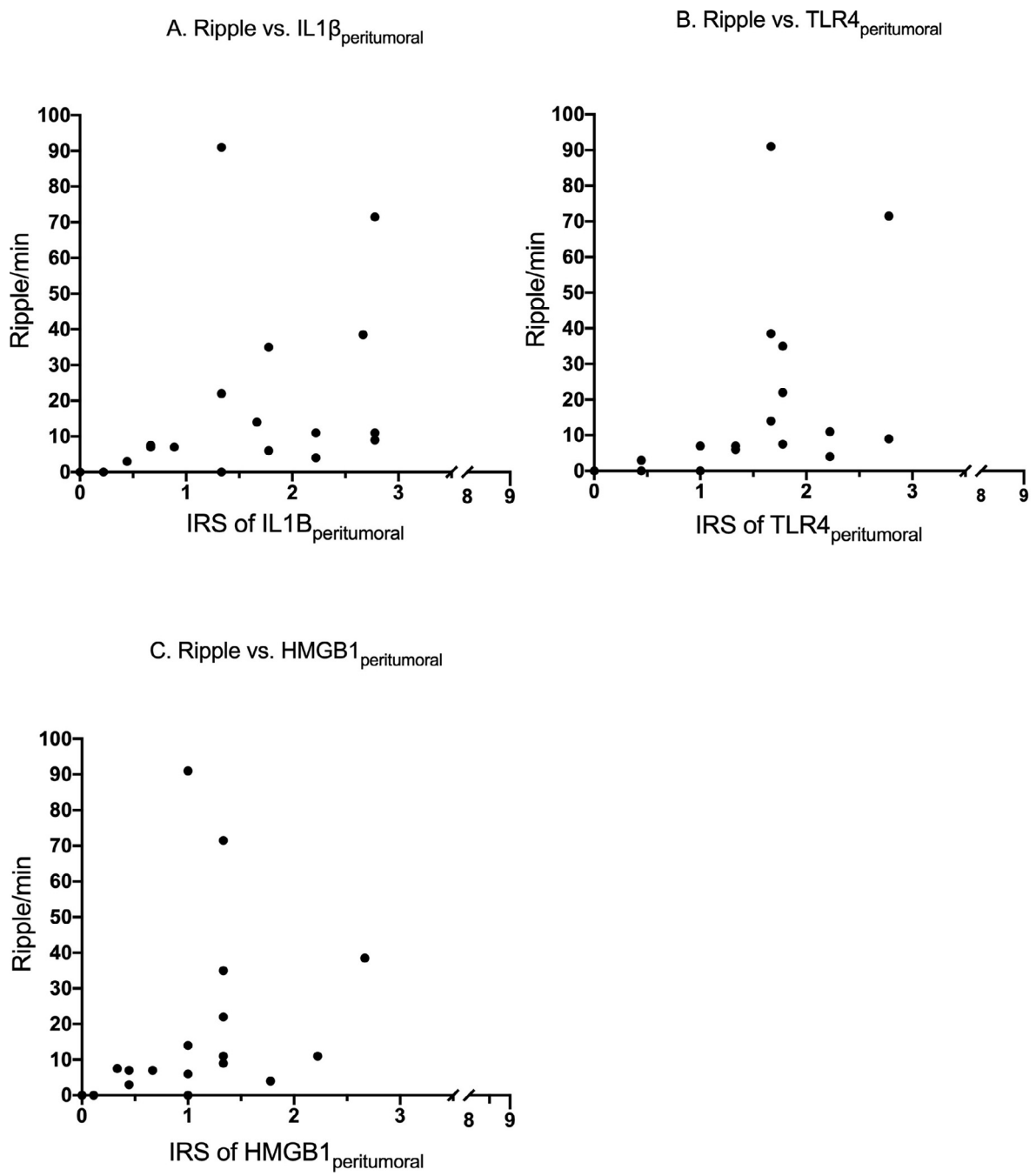

Fig. 6. Scatterplot of ripple rate outside the resected area vs. IL1β, TLR4 and HMGB1 in the peritumoral tissue. The immunoreactivity of inflammatory markers on the x-axis and ripple rates were expressed in number of ripples per minutes on y-axis. Abbreviations: IRS = immunoreactivity score, CD3 = cluster of differentiation 3, IL1β = interleukin 1-beta, TLR4 = toll-like receptor 4, HMGB1 = high mobility group box 1 protein.

populations (Jiruska et al. 2017). We found less FRs than a previous study of our group (Van 't Klooster et al. 2017). The difference in FR rates could be due to the different pathologies that were included in the studies. Different pathologies can show different epileptiform discharges rates and different HFO rates in ECoG. For instance, malformations of cortical development more frequently show continuous spiking patterns and high frequency oscillations than other pathologies (Ferrier et al. 2006; van Klink et al. 2021; Peng et al., 2021). Differences in the number of included bipolar channels could also partially have contributed to the differences in the recorded number of FRs.

Our retrospective study design has several methodological limitations. First, the definition of the location of HFOs being in the tumor or in the resected tissue is not a 100% sure. We defined HFOs in tumor being HFOs recorded in the ioECoG covering the tumor site, but these HFOs are not 'purely' HFOs generated by the tumor. The ioECoG measures cortical activity in a two-dimensional way. In case of a superficial tumor, the ioECoG records mostly the signals of the neoplastic neurons. However, in a deep and more medially located tumor, the ioECoG would consist of signals from the overlaying cortex mixed with signals from the tumor itself. HFOs in the resected tissue outside the tumor should represent the non-

neoplastic tissue which was epileptogenic as it had to be removed during surgery. It is, however, also possible that some of this brain tissue is resected to gain access to the suspected epileptogenic zone. We cannot differentiate these two scenarios. Secondly, we did not correct for the extent of the ioECoG coverage. We choose to analyze the overall ripple rates because the extensiveness of the electrode coverage was at least partially determined by the epileptogenic signal recorded and thus intrinsic to the extent of the epileptogenic zone. To limit potential bias, we calculated the mean number of HFOs if the same brain area was recorded multiple times. Lastly, we did not correct for clinical factors that might have acted as confounders such as seizure duration and higher seizure frequency (Aronica et al. 2005; Boer et al. 2008; Vezzani et al. 2011b) because our data was not suited for multivariate regression models.

This research provides arguments for further investigations into the relationship between HFOs and inflammation. Extending these findings to IDH mutated (diffuse) gliomas, with its specific epileptogenic peritumoral environment (including the presence of 2-hydroxyglutarate), may offer further pathophysiological insights. In future prospective studies, tissue for immunohistological analyses should be sampled at sites where HFOs are recorded to assure a close relation between HFOs and local inflammation. If possible, tissue should also be sampled from a site without HFOs to serve as control sample. The electrode positions have to be marked on the removed brain tissue, e.g. with ink markings or by registration of coordinates with the neuronavigation system. By including the depth of tumors with respect to the grid positions in the MRI reconstructions one could improve accuracy of HFO localization. Intraoperative recordings with high resolution grids could be considered to improve FR sampling. Additional spike analyses might add value in distinguishing between physiological and pathological ripples. Distinction between temporal and extratemporal surgeries is recommended in a larger group of patients.

5. Conclusion

Our work showed that increased ripple rate outside the resected area is correlated with increased immunoreactivity of IL1β/HMGB1/TLR4 in the peritumoral glia cells. CD3-positive T-cell infiltration in the tumor was associated with the local presence of ripples. We found no correlations between fast ripple rates and inflammatory markers, but association between the two could not be excluded due to low numbers of patients with fast ripples. This is the first study to directly compare HFOs and inflammatory markers that contribute to epileptogenesis and provides grounds for further investigations into the relation between HFOs and inflammation. To conclude, HFO rate in the ripple band is associated with inflammatory components such as T-cells and the IL1β/HMGB1/TLR4 pathway. These findings might suggest that synchronized fast firing of hyperexcitable neurons may be a part of the underlying mechanism of ripple generation.

Declaration of Competing Interest

The authors declare that they have no known competing financial interests or personal relationships that could have appeared to influence the work reported in this paper.

Acknowledgements

This work was supported by the European Research Council starting grant 803880 and N.v.K. was supported by the Dutch Brain Foundation (2013-139). Figs. 1 and 2 were created with BioRender.com.

Appendix A. Supplementary material

Supplementary data to this article can be found online at https://doi.org/10.1016/j.clinph.2021.08.025.

References

Aronica E, Gorter JA, Redeker S, Ramkema M, Spliet WGM, Van Rijen PC, et al. Distribution, characterization and clinical significance of microglia in glioneuronal tumours from patients with chronic intractable epilepsy. Neuropathol. Appl. Neurobiol. 2005;31(3):280–91.

Blümcke I, Coras R, Wefers AK, Capper D, Aronica E, Becker A, et al. Review: Challenges in the histopathological classification of ganglioglioma and DNT: microscopic agreement studies and a preliminary genotype-phenotype analysis Available from. Neuropathol. Appl. Neurobiol. 2019;45(2):95–107. http://www.ncbi.nlm.nih.gov/pubmed/30326153.

Blumcke I, Spreafico R, Haaker G, Coras R, Kobow K, Bien CG, et al. Histopathological findings in brain tissue obtained during epilepsy surgery. N. Engl. J. Med. 2017;377(17):1648–56.

Boer K, Jansen F, Nellist M, Redeker S, van den Ouweland AMW, Spliet WGM, et al. Inflammatory processes in cortical tubers and subependymal giant cell tumors of tuberous sclerosis complex. Epilepsy Res. 2008;78(1):7–21.

Bongaarts A, de Jong JM, Broekaart DWM, van Scheppingen J, Anink JJ, Mijnsbergen C, et al. Dysregulation of the MMP/TIMP Proteolytic System in Subependymal Giant Cell Astrocytomas in Patients With Tuberous Sclerosis Complex: Modulation of MMP by MicroRNA-320d In Vitro Available from. J. Neuropathol. Exp. Neurol. 2020;79(7):777–90. http://www.ncbi.nlm.nih.gov/pubmed/32472129.

Burnos S, Hilfiker P, Sürücü O, Scholkmann F, Krayenbühl N, Grunwald T, et al. Human Intracranial High Frequency Oscillations (HFOs) Detected by Automatic Time-Frequency Analysis. Charpier S, editor. PLoS One. 2014;9(4):e94381. Available from: https://dx.plos.org/10.1371/journal.pone.0094381.

Engel J, Cascino GD, Ness PCV, Rasmussen TB, Ojemann LM. Outcome with respect to epileptic seizures. In: Engel J, editor. Surgical treatment of the epilepsies. New York: Raven Press; 1993.

Englot DJ, Berger MS, Barbaro NM, Chang EF. Factors associated with seizure freedom in the surgical resection of glioneuronal tumors. Epilepsia. 2012;53(1):51–7.

Ferrier CH, Aronica E, Leijten FSS, Spliet WGM, Van Huffelen AC, Van Rijen PC, et al. Electrocorticographic discharge patterns in glioneuronal tumors and focal cortical dysplasia. Epilepsia. 2006;47(9):1477–86.

Fujiwara H, Greiner HM, Lee KH, Holland-Bouley KD, Seo JH, Arthur T, et al. Resection of ictal high-frequency oscillations leads to favorable surgical outcome in pediatric epilepsy Available from. Epilepsia. 2012;53(9):1607–17. http://doi.wiley.com/10.1111/j.1528-1167.2012.03629.x.

Giulioni M, Marucci G, Pelliccia V, Gozzo F, Barba C, Didato G, et al. Epilepsy surgery of "low grade epilepsy associated neuroepithelial tumors": A retrospective nationwide Italian study. Epilepsia. 2017;58(11):1832–41.

Graeber MB, Scheithauer BW, Kreutzberg GW. Microglia in brain tumors Available from. Glia. 2002;40(2):252–9. http://www.ncbi.nlm.nih.gov/pubmed/12379912.

Jacobs J, LeVan P, Chander R, Hall J, Dubeau F, Gotman J. Interictal high-frequency oscillations (80–500 Hz) are an indicator of seizure onset areas independent of spikes in the human epileptic brain Available from. Epilepsia. 2008;49(11):1893–907. http://doi.wiley.com/10.1111/j.1528-1167.2008.01656.x.

Jiruska P, Alvarado-Rojas C, Schevon CA, Staba R, Stacey W, Wendling F, et al. Update on the mechanisms and roles of high-frequency oscillations in seizures and epileptic disorders. Epilepsia. 2017;58(8):1330–9.

Lamberink HJ, Otte WM, Blümcke I, Braun KPJ, European Epilepsy Brain Bank writing group, study group, et al. Seizure outcome and use of antiepileptic drugs after epilepsy surgery according to histopathological diagnosis: a retrospective multicentre cohort study. Lancet Neurol. 2020;19(9):748–57. Available from: http://www.ncbi.nlm.nih.gov/pubmed/32822635.

Louis DN, Perry A, Reifenberger G, von Deimling A, Figarella-Branger D, Cavenee WK, et al. The 2016 World Health Organization Classification of Tumors of the Central Nervous System: a summary Available from. Acta Neuropathol. 2016;131(6):803–20. http://www.ncbi.nlm.nih.gov/pubmed/27157931.

Peng SJ, Wong TT, Huang CC, Chang H, Hsieh KL, Tsai ML, et al. Quantitative analysis of intraoperative electrocorticography mirrors histopathology and seizure outcome after epileptic surgery in children. J. Formos Med. Assoc. 2021;120(7):1500–11.

Prabowo AS, van Scheppingen J, Iyer AM, Anink JJ, Spliet WGM, van Rijen PC, et al. Differential expression and clinical significance of three inflammation-related microRNAs in gangliogliomas Available from. J. Neuroinflammation. 2015;12:97. http://www.ncbi.nlm.nih.gov/pubmed/25986346.

Ryvlin P, Cross JH, Rheims S. Epilepsy surgery in children and adults. Lancet Neurol. 2014;13(11):1114–26.

Shimada T, Takemiya T, Sugiura H, Yamagata K. Role of inflammatory mediators in the pathogenesis of epilepsy. Mediators Inflamm. 2014;2014.

Slegers RJ, Blumcke I. Low-grade developmental and epilepsy associated brain tumors: A critical update 2020 Available from. Acta Neuropathol. Commun. 2020;8(1):1–11. http://www.ncbi.nlm.nih.gov/pubmed/32151273.

Thom M, Blümcke I, Aronica E. Long-term epilepsy-associated tumors. Brain Pathol. 2012;22(3):350–79.

Thom M, Liu J, Bongaarts A, Reinten RJ, Paradiso B, Jäger HR, et al. Multinodular and vacuolating neuronal tumors in epilepsy: dysplasia or neoplasia? Available from Brain Pathol. 2018;28(2):155–71. http://www.ncbi.nlm.nih.gov/pubmed/28833756.

van Klink NEC, Zweiphenning WJEM, Ferrier CH, Gosselaar PH, Miller KJ, Aronica E, et al. Can we use intraoperative high-frequency oscillations to guide tumor-related epilepsy surgery? Available from Epilepsia. 2021;62(4):997–1004. http://www.ncbi.nlm.nih.gov/pubmed/33617688.

van 't Klooster MA, van Klink NEC, Zweiphenning WJEM, Leijten FSS, Zelmann R, Ferrier CH, et al. Tailoring epilepsy surgery with fast ripples in the intraoperative electrocorticogram. Ann Neurol. 2017;81(5):664–76. Available from: http://doi.wiley.com/10.1002/ana.24928.

van Vliet EA, Aronica E, Vezzani A, Ravizza T. Review: Neuroinflammatory pathways as treatment targets and biomarker candidates in epilepsy: emerging evidence from preclinical and clinical studies. Neuropathol. Appl. Neurobiol. 2018;44(1):91–111.

Vezzani A, Aronica E, Mazarati A, Pittman QJ. Epilepsy and brain inflammation. Exp. Neurol. 2013;244:11–21.

Vezzani A, French J, Bartfai T, Baram TZ. The role of inflammation in epilepsy. Nat. Rev. Neurol. 2011a;7(1):31–40.

Vezzani A, Friedman A. Brain inflammation as a biomarker in epilepsy. Biomark Med. 2011;5(5):607–14.

Vezzani A, Maroso M, Balosso S, Sanchez MA, Bartfai T. IL-1 receptor/Toll-like receptor signaling in infection, inflammation, stress and neurodegeneration couples hyperexcitability and seizures. Brain Behav Immun. 2011b;25(7):1281–9. Available from: http://www.ncbi.nlm.nih.gov/pubmed/21473909.

Wu JY, Sankar R, Lerner JT, Matsumoto JH, Vinters HV, Mathern GW. Removing interictal fast ripples on electrocorticography linked with seizure freedom in children Available from. Neurology. 2010;75(19):1686–94. https://n.neurology.org/content/75/19/1686.short.

Zijlmans M, Jiruska P, Zelmann R, Leijten FSS, Jefferys JGR, Gotman J. High-frequency oscillations as a new biomarker in epilepsy Available from. Ann. Neurol. 2012;71(2):169–78. http://doi.wiley.com/10.1002/ana.22548.